Argon and krypton Auger spectra induced by ion bombardment of aluminium and silicon surfaces

1994 J. Phys.: Condens. Matter 6 2681

(http://iopscience.iop.org/0953-8984/6/14/006)

J. Phys.: Condens. Matter 6 (1994) 2681–2688. Printed in the UK

Argon and krypton Auger spectra induced by ion bombardment of aluminium and silicon surfaces

A P Nixon, T E Gallon, F Yousif and J A D Matthew
Department of Physics, University of York, Heslington, York YO1 5DD, UK

Received 11 October 1993

Abstract. Measurements are reported of Auger (autoionization) spectra of Ar and Kr produced by bombarding Al and Si substrates with Ar^+ and Kr^+ ions in the 110 eV–5 keV energy range. These are shown to be consistent with the simple Doppler model suggested, for Ne on Al and Si, in a previous paper. Once corrected using the model, the observed Auger energies are shown to correspond to theoretical predictions produced using Dirac–Fock calculations.

1. Introduction

The autoionization spectra of collisionally excited Ne on Al and Si have been discussed in a previous paper [1] and a comprehensive review of the field of ion-induced Auger electron spectroscopy (IAES) has recently been published [2]. In [1], a simple Doppler model was suggested to explain the shift in measured Auger energies with respect to ion-beam energy. The dominant peaks in the data, when modified using the above model, were shown to match the gas-phase data of Olsen and Andersen [3, 4]. The correction used to the measured energy E_M, for an ion beam energy E_I, takes the form

$$E_M = E_A + (4m/M)^{1/2}\sqrt{E_A}\sqrt{E_I - E_L}\cos\theta \tag{1}$$

where m and M are the masses of the electron and emitting atom or ion respectively, E_A is the Auger energy of the emitted electron in the rest frame of the atom, E_L is the energy lost in the collision and excitation process and θ the angle made between the direction of the moving atom and the spectrometer.

It has been known for some time that ions of keV energy approaching a conducting surface often undergo Auger neutralization into their atomic ground state prior to collision with the surface atoms [2]. The electron promotion model produced by Fano and Lichten [5] used to explain the presence of core holes after collision, yields a considerable cross section for the production of multiple excited states. Hence [1] analyses the Ne Auger spectrum in terms of configurations of $2p^43s^2$ or $2p^43s3p$ neutral excited states decaying, via autoionization, to a $2p^5$ ground state.

This paper reports measurements of the autoionizing spectra of Ar and Kr, produced by the interaction of beams of Ar^+ and Kr^+ with the surfaces of Al and Si under UHV conditions. Ion beams in the energy range 110 eV–5 keV were investigated and the spectra show previously unobserved structure at low energy, which is interpreted in terms of autoionization to $3p^5$ and $4p^5$ states respectively.

0953-8984/94/142681+08$19.50

2. Experimental details

For full experimental details the reader is referred to [1]. The angular configurations of the ion gun, spectrometer and sample are all as previously described; they remain fixed throughout the experiment and are such that electrons are detected in the forward scattering direction relative to the incident beam. The specimens were cleaned until the C and O peaks, measured using electron-induced AES, had merged into the background, as described in [1]. All IAES measurements were made in a UHV chamber with a base pressure of 3×10^{-10} mbar; this pressure rose to 2×10^{-6} mbar when Ar or Kr gas was admitted into the ion gun.

3. Results

3.1. Ar on Al and Si

A typical spectrum produced by 500 eV Ar^+ impact on Al is shown in figure 1. As with the Ne IAES data the spectrum is dominated by two large peaks labelled 1 and 2; fine-structure peaks (labelled 2a, 3, 4 and 5) are also observed. At ion-beam energies in the range 110 eV–1 keV the behaviour of the Ar IAES is similar to that of Ne, with a gradual increase in the observed peak energy corresponding to increasing ion-beam energy. As with the Ne data it is possible to apply the Doppler model [1] to peaks 1 and 2 in Ar. Because these peaks become less sharp with increasing beam energy only data below 500 eV are used to produce a least-squares fit to equation (1) for $\cos\theta \simeq 1$ (see table 1), i.e. the emitting atom is moving in a direction close to that of the spectrometer slit. Unlike the IAES observations for Ne, the peaks in the Ar spectrum diminish rapidly for ion energies in excess of 1 keV and merge with the background above 3 keV. This is consistent with the idea that, as the collision energy increases, the excitation of the 2p shell in the target becomes energetically possible and the electron promotion process for the 3p excitation in the projectiles is inhibited. This effect was studied by recording data over the energy range 10–67 eV, covering both the Ar and Al autoionizing spectra. The results, after curve stripping to remove the secondary electron background, are shown in figure 2.

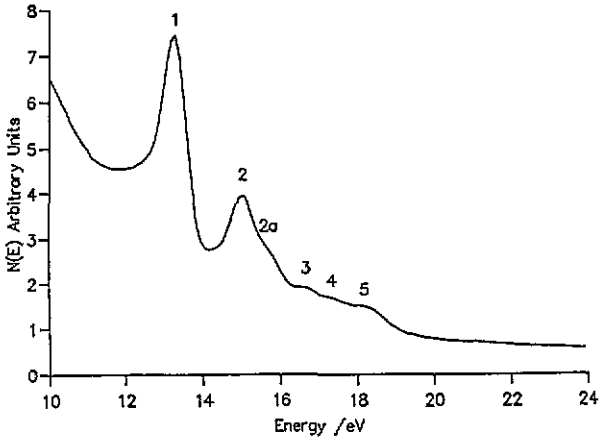

Figure 1. A typical 500 eV Ar^+ excited spectrum on Al before removal of the background.

Table 1. Results of least-squares fit to data for peaks 1 and 2 for ion beams up to 500 eV.

	Peak 1	Peak 2
E_A (eV)	12.0 ± 0.2	13.8 ± 0.2
E_L (eV)	82 ± 18	70 ± 18

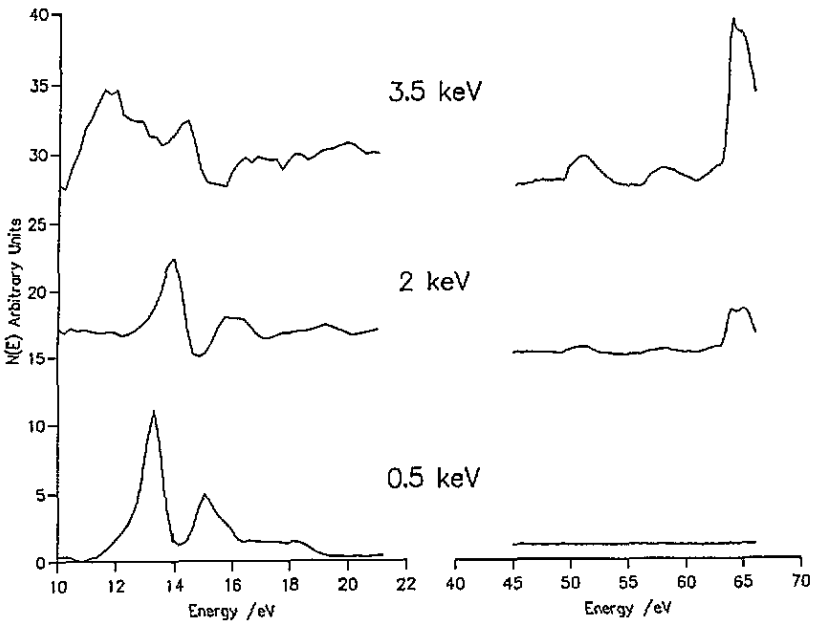

Figure 2. Results of simultaneous observation of Ar and Al line intensities for fixed ion-beam energies of 0.5, 2.0 and 3.5 keV. The intensities of peaks in the 10–20 eV region decrease sharply with increasing energy, but are shown here at comparable signal level for convenience.

Spectra were also recorded for Ar on Si at 500 eV. The two data sets are shown in figure 3 after subtraction of a smooth background and 0.3 eV from the Si data to allow for the difference in work function between Al and Si as with the Ne data. With the exception of peak 0 each of the Ar–Si peaks has a corresponding feature in the Ar–Al spectrum. This is consistent with the observations made for Ne on Al and Si discussed previously, where similar spectra were produced in each case but the relative peak intensities depended on the target. The intensity of the spectrum for Ar–Si is magnified by a factor of four in order to compare with the Ar–Al data as the yield is considerably less for Si. The broad feature in the Si spectrum (shown in figure 3 for Ar–Si) is labelled 0 for convenience rather than to attribute it to the same cause or initial states. A similar broad feature may be present in the Ar–Al spectrum in figure 3, and this increases in relative importance at higher primary ion energy—see figure 2.

The results for Ar on Al and Sr on Si are summarized in table 2. All the peaks (except peak 0, discussed previously), in Ar on Si have corresponding peak in the Ar on Al data with measured energies well within the bounds of experimental error for their energy differences. The absolute error in the corrected value, due to uncertainty in calibration, is probably about 0.5 eV. The error in the differences is less than 0.2 eV; this figure can be evaluated from the model and verified by repeated observation and variation of the parameters used in the

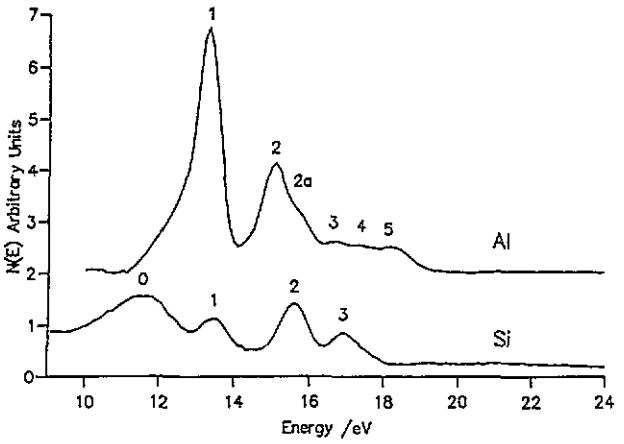

Figure 3. Comparison between Ar electron emission spectra for Al and Si targets after background removal.

Table 2. Comparison of measured and corrected data for Ar on Al and Si.

		Al energy (eV)		Si Energy (eV)	
		Measured	Corrected	Measured	Corrected
	0	9.9 ?	8.7	11.5	9.9
	1	13.3	12.0	13.5	11.8
	2	15.1	13.8	15.6	13.9
Ar	2A	15.8	14.5	—	—
	3	16.7	15.3	16.9	15.2
	4	17.4	16.0	—	—
	5	18.2	16.8	—	—

curve stripping routine.

These peaks were detectable at ion-beam energies down to 110 eV, in the forward-scattering configuration, with the ion beam at glancing incidence to the sample surface, but it was not possible to resolve any features above the background at 100 eV. These spectra seem particularly sensitive to the angle of incidence of the ion beam and this may explain why previous searches, such as that by Zampieri and Baragiola [6], have been unsuccessful in observing MNN transitions in Ar.

3.2. Kr on Al and Si

Although the signal produced by incident Kr ions is of very low intensity it is possible to resolve Kr transitions, similar to those observed for Ar, over a narrow range of energies below 1 keV. In fact the strongest spectra are observed at an ion energy of 800 eV. Data were recorded for Kr on Al and Si as shown in figure 4. As with Ne and Ar, the Kr on Al spectrum is dominated by two peaks (labelled 1 and 2). The Kr on Si spectrum contains a broad feature at low energy (labelled 0) similar to the feature observed in the Ar on Si spectrum. As data are only available over a narrow range of ion energies it was not possible to use the least-squares method previously employed to estimate the unshifted peak energies (E_A) and the energy loss (E_L). However, the value of E_L is not critical when finding E_A; if E_L for Kr is assumed to be less than for Ar (a reasonable assumption, as the binding

energy of the outer shell electrons of Kr will be less than that for Ar) then the influence of E_L on E_A is less than 0.2% and thus it is possible to calculate E_A provided Doppler shifting is occurring.

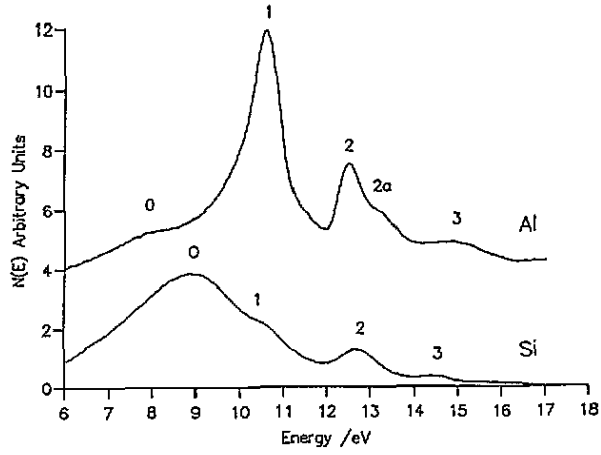

Figure 4. 800 eV Kr IAES spectra for Al and Si in the forward-scattering configuration.

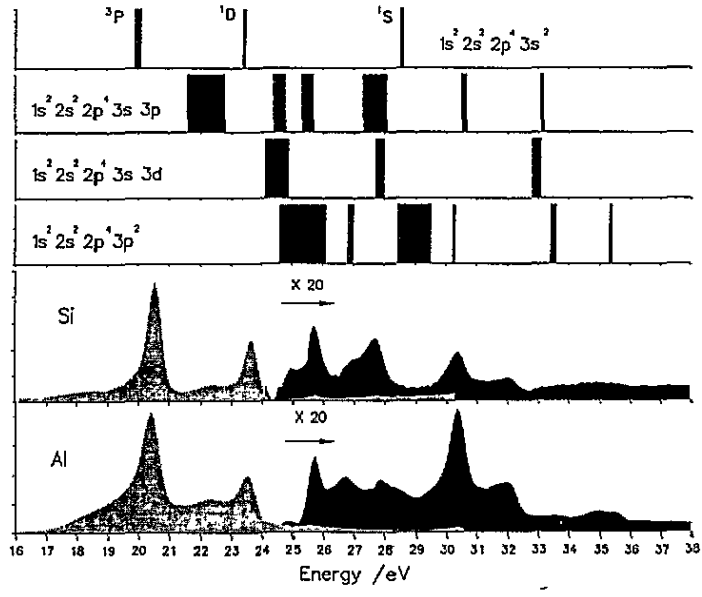

Figure 5. The correspondence between DF calculations and Doppler-corrected IAES spectra for Ne on Si and Al for transitions to the $2p^5$ Ne^+ final state.

The measured energies and the Doppler- and work-function-corrected energies for Kr on Al and Si are summarized in table 3. As described for Ar, the absolute energies of the

Table 3. Measured and corrected data for Kr on Al and Si.

		Al		Si	
		Measured	Corrected	Measured	Corrected
	0	7.8 ?	6.6	8.8	7.3
	1	10.6	9.4	10.6	9.1
Kr	2	12.5	11.3	12.8	11.2
	2A	13.4	12.1	—	—
	3	14.0	12.8	14.5	12.9

corrected data have an uncertainty of about 0.5 eV and the energy differences are within 0.2 eV. Again there is a good correspondence between the corrected peak energies for both Al and Si targets.

4. Theoretical predictions and discussion

It is possible to match many of the Ne, Ar and Kr IAES peaks to theoretical energies predicted by the MCDF (Multi-configurational Dirac–Fock) program of Grant [7]. The method includes Breit corrections to the zero-order energy, as well as allowing for vacuum polarization to first order and a crude approximation to the self-energy.

The results of single-configuration calculations for Ne, Ar and Kr are compared with the corrected experimental data for both targets in figures 5–7, respectively. Some of the configurations include a large number of multiplets, which overlap in energy, and are shown in block form.

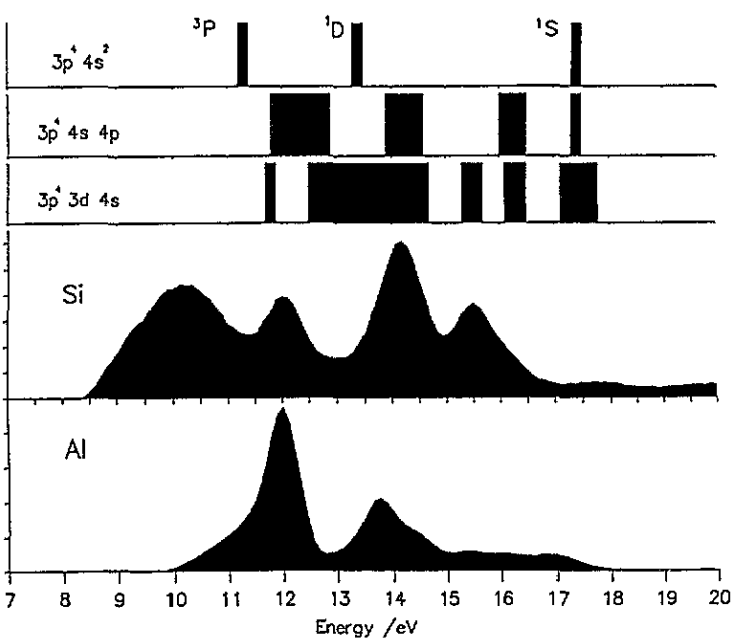

Figure 6. Comparison between DF calculations and Doppler-corrected IAES for Ar on Si and Al for transitions to the Ar^+ $3p^5$ final state.

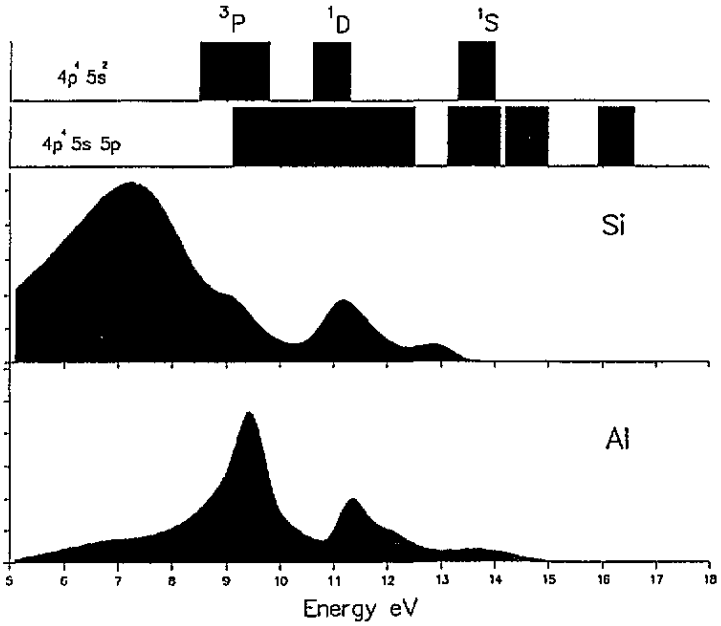

Figure 7. Comparison between DF calculations and Doppler-corrected IAES spectra for Kr on Si and Al for transitions to the Kr^+ $4p^5$ final state.

In figure 5 the smaller Ne peaks above 24 eV have been magnified by a factor of 20 for clarity. In agreement with Gallon and Nixon [1] and Olsen and Andersen [3,4] the strongest features in the Ne spectrum may be unambiguously associated with the ^{3}P and ^{1}D multiplets of the $2p^43s^2$ configuration decaying to the $2p^5$ ground state. The corresponding $3p^44s^2$ $4p^45s^2$ multiplets in Ar and Kr undergo substantial spin–orbit splitting, indicated by the broadening in figures 6 and 7, but correspondence with the main spectral features is again clear—see table 4. In Ne it is possible to make plausible assignments to the remaining features in the spectrum as in the work of Olsen and Andersen [3,4], but the assignments of higher-energy emission features in Ar and Kr are more ill defined. However, the calculation suggests that they have their origin in readily accessible initial-state configurations eg $3p^44s4p$ and $4p^45s5p$.

Table 4. Comparison of DF calculations with corrected experimental data for $np^4(n+1)s^2 \rightarrow np^5$ transitions.

		Theory	experimental
Ne	^{3}P	19.9, 20.1	21.1
	^{1}D	23.4, 23.5	24.3
Ar	^{3}P	11.2, 11.4	12.0
	^{1}D	13.3, 13.5	13.8
Kr	^{3}P	8.5, 9.8	9.4
	^{1}D	10.6, 11.3	11.3

The lower-energy peaks (denoted 0) observed for Ar^+ and Kr^+ on Si and Kr^+ on Al remain to be interpreted. Since these have only been measured in a very narrow primary

energy range it is not clear whether they are Doppler shifted or not. In the case of silicon the observed energies are close to the energies of peak 1 corrected for Doppler shift, i.e. they may correspond to emission from *slow* neutral excited ions near the surface. Alternatively the peaks could involve a totally different kind of decay process. Brenten *et al* [8] have measured electron emission for Ar^+-excited K on W(110): for 1 keV Ar^+ emission at an energy around 3 eV below the ^3P neutral decay dominates and they interpret this as Ar^- $3p^5 4s^2 \rightarrow 3p^6 + e^-$ transitions. However, the formation of excited negative ions is very dependent on the low electronegativity of the surface species, and such a process does not seem likely for an Si surface. The definitive description of this spectral feature requires further investigation.

5. Summary

Autoionizing electron emission of Ar and Kr has been observed in the interaction of Ar^+ and Kr^+ with Al and Si surfaces under UHV conditions. The dominant decay channels are $3p^4 4s^2$ (^3P, ^1D)$\rightarrow 3p^5 + e^-$ and $4p^4 4s^2$ (^3P, ^1D)$\rightarrow 4p^5 + e^-$ respectively, i.e. emission from excited neutrals in the gas phase. This is best achieved at high-angle-of-incidence near-specular geometry where the energy lost in the collision and excitation process is small. It is possible to interpret the shift in Auger energy with respect to ion-beam energy by a simple Doppler model. Although the behaviour is generally similar to that of Ne^+ on Si and Al, autoionizing emission is achieved under more restrictive conditions and in the case of Si is accompanied by an additional emission process whose origin remains to be clarified.

References

[1] Gallon T E and Nixon A P 1992 *J. Phys.: Condens. Matter* 4 9761
[2] Valeri S 1993 *Surf. Sci. Rep.* **17** 85
[3] Olsen J O and Andersen N 1977 *J. Phys. B: At. Mol. Phys.* **10** 101
[4] Andersen N and Olsen J O 1977 *J. Phys. B: At. Mol. Phys.* **10** L719
[5] Fano U and Lichten W 1967 *Phys. Rev.* 14 627
[6] Zampieri G and Baragiola R A 1986 *Phys. Rev.* A 33 588
[7] Grant I P 1972 *Comput. Phys. Commun.* **9** 377
[8] Brenten H, Müller H, Niehaus A and Kempter V 1992 *Surf. Sci.* **278** 183